AAEC/E629

AAEC/E629

AUSTRALIAN ATOMIC ENERGY COMMISSION

RESEARCH ESTABLISHMENT

LUCAS HEIGHTS RESEARCH LABORATORIES

VARIATION OF NEUTRON YIELD FROM A TITANIUM-TRITIDE TARGET DURING DEUTERIUM BEAM BOMBARDMENT

by

A.W. DALTON

H.J. WOODLEY

MAY 1986

ISBN 0 642 59833 9

AUSTRALIAN ATOMIC ENERGY COMMISSION
RESEARCH ESTABLISHMENT

LUCAS HEIGHTS RESEARCH LABORATORIES

VARIATION OF NEUTRON YIELD FROM A TITANIUM-TRITIDE TARGET DURING DEUTERIUM BEAM BOMBARDMENT

by

A.W. DALTON
H.J. WOODLEY

ABSTRACT

In the laboratory simulation of D-T fusion breeder blankets, 14 MeV neutrons are produced by the bombardment of a titanium-tritide target with deuterium ions, using accelerating voltages up to 500 keV and beam currents ranging from micro- to milliamperes. For the accurate determination of tritium breeding ratios in the experimental assemblies, an absolute determination of the total neutron yield over the irradiation period is required.

The theoretical and experimental methods used to determine the ion composition of the deuterium beam, the changing absolute yields, and energy distributions of the neutrons emitted from the target during prolonged irradiation are described, using the AAEC 14 MeV neutron generator as a typical example. The approach is based on a locally developed technique for the analysis of the energy spectra of the charged particle fusion products associated with the neutrons emitted from nuclear interactions in the target during beam bombardment.

Analysis of the measured data identified two ion species in the beam of the neutron generator. It was shown that after a 21-hour irradiation of the target with a 250 μA beam (18.5C) at 200 kV, the neutron output from the D-T reaction dropped from an initial value of 2×10^{10} to 4×10^{8} neutrons per second. The integrated neutron output over this period was estimated to be 2.05×10^{14}, of which about 24 per cent originated from the interaction of monatomic ions and 75 per cent from diatomic ions; less than one per cent arose from the D-D reaction.

National Library of Australia card number and ISBN 0 642 59833 9

The following descriptors have been selected from the INIS Thesaurus to describe the subject content of this report for information retrieval purposes. For further details please refer to IAEA-INIS-12 (INIS: Manual for Indexing) and IAEA-INIS-13 (INIS: Thesaurus) published in Vienna by the International Atomic Energy Agency.

BREEDING BLANKETS; SIMULATION; NEUTRONS; DEUTERON REACTIONS; TRITIUM TARGET; KEV RANGE 100-1000; IRRADIATION; DEUTERIUM IONS; DEUTERIUM BEAMS; IONIC COMPOSITION; EXPERIMENTAL DATA; HELIUM 4; NEUTRON GENERATORS; ION IMPLANTATION; ION SCATTERING ANALYSIS

CONTENTS

1. INTRODUCTION

The tritium required to sustain a fusion reactor system based on the $T(d,n)^4He$ reaction can be produced by the interaction of the neutrons emitted from this reaction with lithium contained in a blanket of material surrounding the plasma. In laboratory experiments designed to establish the economic feasibility of breeding tritium in this manner, the fusion neutrons are produced by the bombardment of a titanium-tritide target with a beam of accelerated deuterium ions; the blanket is represented by an assembly of lithium-bearing material arranged in either 4 or 2 π geometry with respect to the neutron source.

For the accurate determination of tritium breeding ratios in the experimental assemblies, both the tritium production rate and the neutron source strength must be measured with high precision over the duration of the irradiation. In a recent pilot study on the precision of tritium breeding experiments [Brzosko *et al.* 1983], it was concluded that the optimum accuracy would be achieved if the output from the neutron generator was monitored, using the associated particle method [Gunnersen and James 1960; Fewell 1968], and the total tritium production was measured from its beta activity using the liquid scintillation counting technique [Dierckx 1973]. Both of these recommended techniques were used in the present experimental program. Details are given of the accurate determination of the neutron output during tritium breeding experiments.

Because the beta decay energy is so low ($\sim$ 18 keV) and the decay constant of such small magnitude (1.79×10^{-9} s^{-1}), high integrated neutron outputs of the order of 10^{15} are required to obtain an acceptable statistical accuracy for the total amount of tritium produced throughout the blanket volume. The AAEC 14 MeV neutron generator, operating at 200 kV with beam currents of 250 μA, yields 2×10^{10} neutrons per second with a new target and is typical of the machines used in these experiments. To achieve the high total neutron output required for the measurement of tritium production using this method, long irradiation times (*e.g.* several weeks) are required; during this time a number of new targets may be consumed.

During a typical irradiation with such neutron generators, two phenomena occur which produce significant variations in the neutron output. First, evaporation of tritium from the target, as a consequence of the energy deposited by the deuterium beam, produces a decreasing output of 14 MeV neutrons under steady operating conditions. Second, interaction of the beam with implanted deuterium ions in the target produces neutrons of much lower mean energy (2.8 MeV). The effects of both phenomena on the absolute neutron yield can be further complicated by the existence of more than one type of ion in the deuterium beam. The errors produced by these effects increase with the duration of the beam irradiation.

In the associated particle technique, the integrated neutron output from the target is determined by collecting the charged alpha particles emitted with the neutrons from the reaction

$$D + T = {}^4He\ (3.5\ MeV) + n\ (14.1\ MeV)$$

in a small solid angle. The counts in the alpha particle energy spectrum accumulated during the irradiation period are integrated over 4π to determine the total neutron yield [Benveniste and Zenger 1954]. The presence of different ion species in the beam is observed as peaks in the energy spectrum of the emitted alpha particles. From the area under these peaks, it is possible to determine the neutron yields from the $T(d,n)^4He$ reaction arising from the different ion species.

As a consequence of deuterium implantation, two additional fusion reactions can occur within the target:

$$D + D = T\ (1.01\ MeV) + p\ (3.02\ MeV);$$

$$D + D = {}^3He\ (0.82\ MeV) + n\ (2.45\ MeV).$$

The charged particles from both reactions are also collected by the solid state detector and their energy spectra superposed on that of the alpha particles from the D-T reaction. Because the energies of these particles differ from those of the alphas, it is also possible to determine their neutron output from the measured energy spectra.

This report also describes the experimental procedures and analytical techniques used to determine both the total intensity and energy distribution of the neutron output from a titanium-tritide target as a function of deuterium beam bombardment. In this analysis the separate contributions arising from the interaction of each type of deuterium ion in the beam, with both the tritium and implanted deuterium in target, are determined.

2. EXPERIMENTAL DETAILS

2.1 Neutron Generator

The 14 MeV neutron generator installed at Lucas Heights (figure 1) is typical of the machines used for integral tritium breeding experiments. Similar generators have been reported by Bachmann *et al.* [1978] at Karlsruhe, in the Federal Republic of Germany (FRG), Hemmendinager *et al.* [1979] at Los Alamos, Herzing *et al.* [1976] at Juelich, FRG, and Takahashi *et al.* [1984] at the Japan Atomic Energy Research Institute (JAERI).

The AAEC generator uses a Penning ion source to supply the ionised deuterium gas to the accelerating section. This type of source is known to produce a higher proportion of diatomic ions than the radiofrequency sources used in most other generators. In common with many other machines, a thick titanium tritide target is used to optimise the neutron output. The target thickness of about 4 μm is much greater than the range of the accelerated deuterium ions (section 4) and contains a tritium concentration of 4.56×10^{22} cm^{-3}. The area of the beam on the target is 100 mm^2; when operated at 250 μA and 200 kV, the measured yield was 2×10^{10} neutrons per second.

To facilitate the continuous measurement of the neutron output from the accelerator during integral experiments, a commercially available solid-state detector was fitted to the existing flight tube assembly. With this detector, the charged particles produced by the D-T and D-D reactions in the target were collected at a backward angle of 135° in a solid angle of 3.45×10^{-8} sr (figure 2). The latter was defined by a 4.64 mm diameter window located in front of the detector, 700 mm from the target.

2.2 Surface Barrier Detector

The Canberra Instruments type PD-25-18-100 solid state detector is biased at 47 V, and has a depletion depth of 100 μm. This depth is sufficient to stop alpha particles with energies up to 12 MeV.

Deuterium ions backscattered by the target produce a background contribution in the solid-state detector which increases markedly with rises in beam energy and current. This can be completely eliminated by positioning an aluminium foil, of thickness 205 μg cm^{-2}, between the target and the detector.

2.3 Data Acquisition and Analysis

The signals from the surface barrier detector are fed through a preamplifier located close to the detector to a Canberra Instruments model 2021 amplifier in the control room, about 20 m away. The output from the amplifier is fed into a Canberra Instruments model 8075 analogue-to-digital converter (ADC) then into the 4 kbyte memory of a Canberra Instruments series 40 multichannel analyser (MCA). For all measurements, a 1 kbyte channel display was used to allow up to four pulse height spectra to be stored in the memory.

For detailed analysis, the data were transferred as individual files to the floppy disc storage of a SIRIUS microcomputer. Locally written software was used to process the archival data, perform such analyses as smoothing, fitting linear or exponential background corrections, search for spectral peaks, calculate areas under peak distributions, fit Gaussian curves, and strip one spectrum from another.

3. THEORY

3.1 Factors Affecting Neutron Output

During long beam irradiations, the neutron output can decrease markedly as a consequence of the loss of tritium from the target. The latter results from the heat generated in the target by the deceleration of the deuterium ions. The rate at which tritium diffuses from the target depends on the balance between the rates at which heat is deposited by the beam and removed by the cooling system. As a consequence, the neutron output eventually drops to such a low level that it becomes necessary to replace the target; the timing of this change is arbitrary, being a compromise between target replacement cost and the rate at which the required neutron fluence is being accumulated. Target changes every five hours have been reported [Brzosko *et al.* 1983].

Another factor contributing to variations in the neutron output is the implantation of deuterium atoms in the target. The concentrations at any given time will be a dynamic balance between the implantation rate and the rate of 'boiling off'. Deuterium atoms implanted in the target result in the generation of neutrons from the D(d,n)^{3}He reaction which have a much lower mean energy ($\sim$ 2.8 MeV) and a more anisotropic angular distribution; fortunately, the cross section at these energies is only about one per cent of that for the T(d,n)^{4}He reaction [Tuck 1961].

A third factor likely to produce variations in the neutron output is the presence of multiple deuterium ion species in the beam. Most ion sources produce singly charged deuterium ions which contain one or more deuterium atoms, the relative proportions of which depend on the ion source. On impact with the target, the heavier ions split into monatomic ions. Hence the energies of the monatomic ions thus produced will be integral fractions of the energy of the source ions.

Because the depth of penetration is greater for the higher energy deuterium ions, the depletion profile of tritium varies with both time and depth below the target surface. Thus the proportion of 14 MeV neutrons originating from the interaction of the different ion species with the tritium in the target will also vary continuously throughout the beam irradiation. For the same reasons, the concentration profile for deuterium implantation will also vary with the time of irradiation and depth below the target surface, producing a continuously varying yield of 2.8 MeV neutrons from the D(d,n)T reaction.

3.2 Neutron Yield

The total thick target yield of neutrons, $Y_n(E_d)$ per incident monatomic deuterium ion of energy E_d (adapted from equation (8) of Benveniste and Zenger [1954]), is given by

$$Y_n(E_d) = 4\pi \int_0^{E_d} \frac{N d\sigma(e)/dw'}{de/dx}\, de \quad , \tag{3.1}$$

where N is the number of tritium nuclei cm^{-3}, $d\sigma(e)/dw'$ is the centre of mass differential cross section, w' is the solid angle in the centre of mass, and de/dx is the rate of energy loss by deuterium ions in the target.

An absolute determination of $Y_n(E_d)$ is obtained, by scaling up to 4π sr the number of alphas per incident deuterium ion, $c(E_d)$, collected by the detector in a well defined solid angle, w, using the following equations (based on an analysis by Fewell [1968]):

$$Y_a(E_d) = (4\pi/w).c(E_d).R_a(E_d) \quad ; \tag{3.2}$$

$$Y_n(E_d) = Y_a(E_d) \quad ; \text{ and} \tag{3.3}$$

$$R_a(E_d) = P_a(E_d, w', CM)/P_a(E_d, w, \theta) \quad , \tag{3.4}$$

where $R_a(E_d)$ is the anisotropic correction factor for deuterium ions of incident energy E_d, $P_a(E_d,w,\theta)$ is the probability that the alpha particle is produced in the target by a deuterium ion of energy E_d and is emitted into the solid angle w at an angle θ' with respect to the incident deuterium beam, and $P_a(E_d,w',CM)$ is the same probability in the centre of mass (CM) system. Because the deuterium ions have a finite probability of interacting throughout a region defined by its range in the target material, $R_a(E_d)$ is dependent not only on the incident deuterium ion energy but also on the depth profile of the tritium concentration in the target.

Similar relationships hold for the D(d,n)^{3}He reaction but from the experimental point of view, the relatively low energy of the ^{3}He particles makes it difficult to discriminate their signals from the high background at the lower energy end of the spectrum. Hence it is not possible to monitor the neutron output from this reaction directly. The neutron yield from the D-D reaction is therefore determined from a measurement of the energy spectrum of the protons from the second reaction D(d,t)p using the conversion factors reported by Tuck [1961].

3.3 Spectrum Analysis

During beam irradiation, the atomic concentrations of tritium and deuterium in the target vary with the duration of the bombardment. The number of alpha particles, $c(E_d,t)$, produced per monatomic deuterium ion of incident energy E_d, which are collected by the detector is proportional to the atomic concentration of tritium,N(t), in the target at time t, hence related to zero time:

$$c(E_d,t) = c(E_d).N(t)/N_o \quad , \tag{3.5}$$

where N_o is the tritium concentration and $c(E_d)$ the yield at time zero. For a beam current of 1 A, alpha particles enter the detector at a rate given by

$$C(E_d,t) = (I/e)c(E_d).N(t)/N_o \quad . \tag{3.6}$$

In practice, this relationship is complicated by the presence in the beam of multiple deuterium ion species having different incident energies within the target, and the differential depletion of tritium with depth of penetration which they produce; consequently, separate equations are required to describe each condition. The equations used are given in section 4. Similar relationships hold for the number of protons produced by interaction of the incident deuterium ions with those implanted in the target.

The concentration depth profile of both materials can be determined from an analysis of the energy spectrum of the charged particles emitted during beam irradiation. If the time for the accumulation of the spectrum is short compared to the total irradiation time, the changes in the concentration profiles can be measured.

3.4 Energy of the Detected Charged Particles

The energy, E_3, of a charged particle emitted in a two-bodied nuclear reaction at an angle θ to the beam in the laboratory frame of reference [Mayer and Rimini 1973] is

$$E_3 = A.E_T.(\cos\theta + (B/A - \sin^2\theta)^{1/2})^2; \tag{3.7}$$

where

$$A = M_1.M_3.(E_1/E_3)/(M_1 + M_2)(M_3 + M_4),$$

$$B = M_2.M_4.(1 + M_1.Q/M_2.E_T)/(M_1 + M_2)(M_3 + M_4),$$

$$E_T = E_1 + Q, \text{ and}$$

$$Q = (M_1 + M_2 - M_3 - M_4).c^2.$$

Subscripts 1 and 2 refer to the incident and target nuclei, and 3 and 4 to the detected and undetected particles. For the T(d,n)^{4}He reaction, they refer to deuteron, triton, alpha and neutron, respectively, and for the D(d,p)^{3}He reaction, to incident and target deuteron, proton and ^{3}He particle, respectively.

Deuterium ions incident on the target lose energy and come to rest in the material at a depth which depends on the incident energy and the stopping characteristics of the material [Littmark and Ziegler 1975], hence they will be different for different ion species. In the beam-target geometry of figure 1, deuterium ions enter the target normal to the surface. Their energy $E_d(x)$ at distance x below the surface (based on an analysis of Cowgill [1977]) is given by

$$E_d(x) = E_1 - S_d.x \ , \tag{3.8}$$

where S_d is the stopping power of the target material for deuterium ions. Over the deuteron energy range of the present series of experiments (0 to 200 keV), the range of deuterium ions in the target is almost linear, and it is assumed that in all of the following analyses, S_d is constant.

On escape from the target, the charged particles created with energy E_3 lose energy at a rate determined by the stopping power, S_a, of the target material and emerge from the target at an angle θ with an energy $E_a(x)$:

$$E_a(x) = E_3 - S_a.x' \ , \tag{3.9}$$

where $x' = -x \sec\theta$, the charged particle path length.

The maximum distance traversed by the charged reaction products will be 1.17 secant (135°) μm, where 1.17 μm is the range for deuterium ions of maximum energy (200 keV) in the target. The charged particles, *e.g.* alphas from the T(d,n)^{4}He reaction and protons from the D(d,n)^{3}He reaction, will have energies of about 3 MeV. Over the range of traverses in the target, the respective stopping powers for these particles will each be approximately constant; this is assumed in the following analysis.

The net depth-dependent energy dispersion of the emerging particles is obtained by combining equations 3.7 to 3.9 and differentiating with respect to x :

$$\frac{dE_a}{dx} = -S_a.\sec\theta - \frac{S_d.dE_3}{dE_d} \ . \tag{3.10}$$

For the backward angles used in the present experimental arrangement, differentiation of equation 3.7 shows that dE_3/dE_d is negative, hence the energy loss of the charged reaction particles reduces the energy spread of the detected particles. The mean energy and spread of the energies with which the charged particles emerge from the target in the direction of the detector are obtained by integrating the above equations over the range of the incident deuterium ions in the target.

4. RESULTS

4.1 Identification of Ion Species

Although different deuterium ion species are produced in the source, they arrive at the target with the same kinetic energy, having experienced the same accelerating voltage. On first impact with the target, any D_2 or D_3 ions will split into monatomic ions of one half and one third of the incident energy, respectively, so the alpha particles produced in the $T(D,n)^4He$ reaction have different energies (equation 3.7), the differences being greatest for backward angles.

The energy spectrum of alpha particles obtained from a new target irradiated with a 50 μA beam at 200 kV for 100 seconds is shown in figure 3. Only two peaks were visually resolved, indicating the presence of two deuterium ion species. These were identified as monatomic (D_1) and diatomic (D_2) ions from their position on the calibrated energy scale of the MCA. A detailed numerical analysis of the spectrum showed that the relative contribution to the neutron output from D_3 was less than one per cent indicating that the proportion of the latter ions was less than 5 per cent of the total beam. In the analysis of subsequent data, the fraction of triatomic ions was assumed to be negligible.

The ratio of counts in the two peak distributions showed that the neutron yield from diatomic ions was about five times (4.7) that from monatomic ions. On first contact with the target, the incident diatomic ions split into two monatomic ions, each having an energy of 100 keV. Using the technique described by Loebenstein and Gazit [1973], the relative neutron yields from the $T(d,n)^4He$ reaction for monatomic deuterium ions of 100 and 200 keV were found to be about 1:4. The observed neutron yields from the two different ion species showed that diatomic ions constituted 92 per cent of the total beam (diatomic to monatomic ratio 11.5:1).

4.2 Effects of Beam Irradiation

A 250 μA beam at 200 kV, focused onto a 100 mm^2 area of the target, produced a power dissipation of 50 W cm^{-2} within the target and an ion implantation rate (combined monatomic and diatomic) of $1.56 \times 10^{15} s^{-1}\ cm^{-2}$. Because the ranges of the deuterium ions in the target are very small (0.59 and 1.17 μm at 100 and 200 keV, respectively [Littmark and Zanger 1974]), the power density and ion implantation are extremely high over these ranges. The average effects produced in the two regions defined by the ranges in the target of the ions from the D_2 and D_1 components of the beam are given in table 1. These values show that most of the energy and ion deposition arises from the diatomic ions and occurs in region 1.

TABLE 1
POWER DENSITIES AND ION IMPLANTATION RATES IN THE TARGET

Region	Boundaries (μm)	Energy Deposition (W cm^{-3})		Deuterium Implantation (atom s^{-1} cm^{-3})	
		Diatomic	Monatomic	Diatomic	Monatomic
1	0.00-0.59	780	34	4.84×10^{19}	
2	0.59-1.17		34		2.12×10^{18}

The energy deposition results in local heating near the target surface and, in spite of efficient cooling at the rear of the copper substrate supporting the target (the titanium-tritide layer), tritium is 'boiled off' from the heated region at a rate which increases with the rate of energy deposition. Because this is greatest in region 1, the loss (bum-up) of tritium is also greatest in this region. As a result, the neutron yield from the two ion species varies differentially with beam irradiation, affecting both the total yield and the energy distribution of the neutrons emitted from the target.

Similarly, the rate at which deuterium atoms are implanted in the target is greatest in region 1; their instantaneous concentration is a balance between the rate of build-up and the rate of boiling off. Because of deuterium implantation in the target neutrons, which have a markedly different energy distribution, can be produced *via* the $D(d,n)^3He$ reaction, as illustrated in table 2, with a yield which depends on the concentration profile of the implanted deuterium ions.

TABLE 2
NEUTRON ENERGY DISTRIBUTIONS FROM IRRADIATED TARGETS

Reaction	Deuterium Ion Energy (keV)	Emitted Neutrons Angle (°)	Energy (MeV)	Spread (keV)
$T(d,n)^4He$	200	0	14.87	380
		180	13.40	270
	100	0	14.70	220
		180	13.55	170
$D(d,n)^3He$	100	0	2.78	133
		180	2.19	87

4.3 Mean Energy and Spread of Detected Charged Particles

The energy of the alpha particles produced in the $T(d,n)^4He$ reaction for the different ions was obtained using equation 3.7. Both the mean and spread in energy of the alpha particles incident on the solid-state detector are affected by

(a) energy losses of the charged particles in the target;

(b) straggling in the Al foil; and

(c) angular acceptance and energy resolution of the detector.

The effects produced in the target (table 3) were obtained by a spatial integration of equations 3.6, 3.7 and 3.10 over the ranges of the respective incident deuterium ions in the target, assuming that a nuclear reaction was equally probable over the whole of the range.

TABLE 3
ENERGY OF ALPHA PARTICLES FROM THE D-T REACTION

Incident Ions			Alpha Particles		
			Reaction	Exit from Target	
Species	Energy (MeV)	Range (μm)	Energy (MeV)	Energy (MeV)	Spread (keV)
D_1	200	1.17	3.027	2.806	60
D_2	100	0.59	3.129	3.060	30

The total cross section for the $D(d,n)^3He$ reaction is a factor of about 100 less than that of the $T(d,n)^4He$ reaction [Tuck 1961] at the beam energies used, hence the only significant contribution to the neutron output from the D-D reaction should arise from the deuterium implanted with the diatomic ions because they constitute 92 per cent of the beam. The energy of the protons from the associated D-D reaction can be similarly calculated; those arising from diatomic ions (D_2) at an angle of 135° have a mean energy at onset of 2.81 MeV and 2.78 MeV on exit from target; the spread of the latter is about 20 keV.

The energy losses in the 205 $\mu g\ cm^{-2}$ aluminium window shielding the detector were 0.166 ± 0.019 MeV for the 3.06 MeV alpha particles from the D-T reaction and 0.018 ± 0.010 MeV for the 2.81 MeV protons from the D-D reaction [Ziegler 1974]. Account was taken of these energy losses in the spectral analyses.

The energy resolution of the surface barrier detector used in the present experiments was 18 keV. Its angle of acceptance for charged particles produced over the area of the detector (4.64 mm diameter) from an irradiated target area (100 mm^2) was ± 0.6°. This produced an energy spread of about 0.2 keV.

4.4 Neutron Yield

In the calculation of the neutron yield, the varying tritium concentration depth profile with irradiation was represented crudely in terms of the mean tritium densities in two regions only, *i.e.* $N_1(t)$ in region 1 and $N_2(t)$ in region 2 at time t. Hence the arrival rates of alpha particles, $C_1(100,t)$, from the 100 keV ions, and $C_1(200,t)$ from the 200 keV ions, at the detector at time t from interactions in region 1, are represented by

$$C_1(100,t) = 2.(m\ I/e).c(100)\ N_1(t)/N_o \quad , \tag{4.1}$$

$$C_1(200,t) = ((1-m)\ I/e).(c(200)-c(100)).N_1(t)/N_o \quad , \tag{4.2}$$

where m is the diatomic ion beam fraction (E_d = 100 keV) and, from interactions in region 2,

$$C_2(200,t) = ((1-m)\ I/e)\ c(100)\ N_2(t)/N_o \tag{4.3}$$

The individual neutron yields for each ion species and each region were obtained by combining the above equations with equations 3.2 and 3.3; values for $c(E_d)$ and $R_a(E_d)$ were taken from Benveniste and Zenger [1954]. The total neutron output from a new target for a 250 μA, 200 kV beam was 2 x 10^{10} s^{-1} (8 $\times$ 10^7 μC^{-1}), 85.3 per cent of which was produced by diatomic ions. The reaction rate in region 1 (the sum of equations 4.1 and 4.2) exceeded that in region 2 (equation 4.3) by a factor of 24.

The atomic concentrations of tritium and deuterium in the target were obtained from an analysis of the charged particle energy spectra measured in short test runs (50 mC at 200 kV) spread over the total irradiation period. A sample of the measured spectra is shown in figure 4.

The atomic concentrations of tritium and deuterium at each stage of the irradiation determine the energy spectra of the alpha particles and protons emitted in the $T(d,n)^4He$ and $D(d,p)^3He$ reactions, respectively. The peak labelled D_1 in figure 4 is actually two peaks, one corresponding to alpha particles from the D-T reaction and the other to protons from the D-D reaction. The contributions from regions 1 and 2 were obtained by an iterative solution of a combined set of equations 4.1, 4.2 and 4.3 for both of these reactions. In these calculations, it was assumed that D-D reactions in region 2 were negligible (table 1) and that in region 1 they occurred only as a result of the interaction of the incident 200 keV monatomic deuterium ions with the previously implanted deuterium from the diatomic ions.

It was found that the tritium concentration decreased progressively with beam irradiation in both regions, the effect being greater in region 1. After a bombardment of 18.5 C cm^{-2}, the mean tritium densities had fallen from an initial uniform target value of 4.56 $\times$ 10^{22} to 9.13 $\times$ 10^{20} in region 1 and to 8.91 $\times$ 10^{21} atoms per cm^2 in region 2, respectively. The concentrations of implanted deuterium in region 1 built up during the beam irradiation, attaining a steady state value of about 4.68 $\times$ 10^{21} atoms per cm^3 after an irradiation of 5 C cm^{-2}.

The varying contributions to the neutron output throughout the target irradiation arising from the $T(d,n)^4He$ and $D(d,n)^3He$ reactions were obtained from the calculated tritium and deuterium concentrations in the target, using equations 3.2 and 3.3. After the 18.5 C bombardment, the total neutron output had fallen from its initial value of 2 $\times$ 10^{10} to 4 $\times$ 10^8 s^{-1}. The variation of the neutron output during this time is shown in figure 5. At the end of the irradiation, about 68 per cent of the total neutrons arose from the interaction of diatomic ions in the D-T reaction and less than 10 per cent from the D-D reaction. The total integrated neutron output over the irradiation period was estimated to be 2.05 $\times$ 10^{14} neutrons, of which 24 per cent arose from the interaction of monatomic deuterium ions in the D-T reaction and 74.9 per cent from diatomic ions; the overall contribution from the D-D reaction was about 0.7 per cent.

5. DISCUSSION AND CONCLUSIONS

Application of experimental and theoretical techniques to the operation of a 14 MeV neutron generator located at Lucas Heights has demonstrated the relative importance of the various factors influencing its neutron output. However, the details of the method are not specific to the latter and therefore the analysis could be applied equally well to any neutron generator working on similar principles.

For our machine, it has been shown that the variation of tritium concentration in the target produced marked changes in the neutron output during the useful life of the target. Two deuterium ion species were identified in the beam and their effect on the neutron output as a result of the variation which they produced in the tritium concentration with depth below the target surface was also shown to be significant (figure 5).

The calculations highlighted the importance of including the implantation of deuterium in the target in the analysis. The neutron output from the D-D reaction, although shown to be relatively small, has a markedly different energy distribution to those produced in the D-T reaction (table 2). In the analysis of tritium breeding experiments, it is important to note that the cross sections of ^6Li for the production of tritium by neutrons from the D-D reaction are seven or eight times larger than those from the D-T reaction. Also the mean neutron energy from the D-D reaction lies below the threshold of the tritium production reaction in ^7Li. Significant error in the tritium breeding ratios would result if no account was taken of the D-D reaction in the analysis of the energy spectra.

Although it is possible to estimate the total neutron yield and its changing energy distribution during the lifetime of the target, such calculations are time-consuming and limit the final accuracy that can be achieved in the tritium breeding experiments. Greater accuracy would be obtained if

(a) the diatomic component could be removed from the target and the monatomic component increased to produce the same neutron yield, and/or

(b) a more sensitive method were used to measure the tritium production rates in the simulated breeder blankets.

The present neutron output could be achieved for a beam which contained only monatomic ions with a beam current of 140 μA at 200 kV. Because there would be only one type of ion, the energy would be uniformly deposited in regions 1 and 2, that in region 1 being a factor of 3.3 less than at present, *i.e.* down to 238 from 814 W cm^{-3}; the target half-life would increase from 1.5 to almost 5 C cm^{-2}. The complications arising from the D-D neutrons would also be much less significant because the implantation would be concentrated only in region 2 and its magnitude reduced from 4.84×10^{19} to 1.06×10^{19} atom s^{-1} cm^{-3}.

A method for producing this type of beam with the present ion source and accelerating tube is being investigated. Calculations are under way to determine the feasibility of separating the two ion species, and on focusing the monatomic ion component onto the target using magnetic and electrostatic deflection. The possibilities of increasing the monatomic component by increasing either the supply of gas to the ion source or the gas to ion conversion efficiency is also being investigated. The latter does not seem unreasonable in view of its present value of 0.28 per cent as estimated from the measurements of the gas flow rate to the ion pump and the integrated ion current on target.

An increase in the sensitivity of tritium detection would reduce the neutron output required to achieve the desired experimental accuracy in the determination of breeding ratios. A method based on the electronic detection of tritium breeding using lithium glass scintillators is at the stage of being tested in the breeding blanket assembly. The sensitivity of detection is expected to be between 10 and 100 times greater than that of the chemical separation technique. Here, the effect of tritium depletion and deuterium implantation on the experimental accuracy would be diminished by a similar factor.

6. ACKNOWLEDGEMENTS

Our thanks are due to the professional and technical staff involved in the present project; to R.J. Blevins and W.J. Crawford for assistance with the experimental work and operation of the 200 keV Activitron neutron generator respectively; to Dr J.W. Boldeman and J.P. Fallon for invaluable help in setting up the neutron monitoring system; to Dr D.D. Cohen of the Australian Institute of Nuclear Science and Engineering for helpful discussions relating to ion implantation; and to G.W.K. Ford for continuous encouragement and support.

7. REFERENCES

Bachmann, H., Fritscher, U., Kappler, F.W., Rusch, D., Werle, H., Wiese, H.W. [1978] - Neutron spectra and tritium production measurements in a lithium sphere to check fusion reactor blanket calculations. *Nucl. Sci. Eng.*, 67:74-84.

Benveniste, J., Zenger, J. [1954] - Information on the neutrons produced in the $T(d,n)^4He$. UCRL-4266.

Brzosko, J.S., Ingrosso, L., Robouch, B.V. [1983] - Depression of the nuclear properties of fusion reactor blankets by inhomogeneities, Proc. *9th European Conf. Controlled Fusion and Plasma Physics*, Aachen, 12-15 September. ECA-7D, part II, pp.543-549.

Cowgill, D.F. [1977] - Dynamic implant profiling by low-energy nuclear reaction spectroscopy. *Nucl. Instrum. Methods*, 145:507-516.

Dierckx, R. [1973] - Direct tritium production measurement in irradiated lithium. *Nucl. Instrum. Methods*, 107:397-398.

Fewell, T.R. [1968] - An evaluation of the alpha counting technique for determining 14-MeV yields. *Nucl. Instrum. Methods*, 61:61-71.

Gunnersen, E.M., James, G. [1960] - On the efficiency of the reaction $H^3(d,n)He^4$ in titanium tritide bombarded with deuterons. *Nucl. Instrum. Methods*, 8:173-184.

Hemmendinger, A., Ragan, C.E., Wallace, J.M. [1979] - Tritium production in a sphere of ^{6}LiD irradiated by 14-MeV neutrons. *Nucl. Sci. Eng.*, 70:274-280.

Herzing, R., Kuijpers, L., Cloth, P., Filges, D., Hecker, R., Kirch, N. [1976] - Experimental and theoretical investigations of tritium production in a controlled thermonuclear reactor blanket model. *Nucl. Sci. Eng.*, 60:169-175.

Hiraoka, T., Maekawa, H., Seki, Y., Hirota, J. [1974] - Integral experiments on a spherical lithium metal blanket system. *Proc. IAEA Workshop on Fusion Reactor Design Problems*, Culham, UK, 29 January to 15 February. *Nuclear Fusion, Special Supplement*, pp.363-376, IAEA, Vienna.

Littmark, U., Ziegler, J.F. [1975] - Range Distributions for Energetic Ions in All Elements. Pergamon Press, New York, Vol 6.

Loebenstein, H.M., Gazit, Y. [1973] - A simple beam charge monitor for neutron generators. *Nucl. Instrum. Methods*, 108:387-388.

Mayer, J.W., Rimini, E. [1973] - Ion Beam Handbook for Material Analysis. Academic Press, New York.

Takahashi, A., Yugami, K., Kohno, K., Ishigaki, N. [1984] - Measurements of tritium breeding ratios in lithium slabs using rotating target neutron source. Proc. *13th Symp. Fusion Technology*, Varese, Italy, 24-28 September, pp.1-5.

Tuck, J.L. [1961] - Thermonuclear reaction rates. *Nucl. Fusion*, 1:201-202.

Ziegler, J.F. [1974] - Stopping Cross Sections for Energetic Ions in All Elements. Pergamon Press, New York, Vol 5.

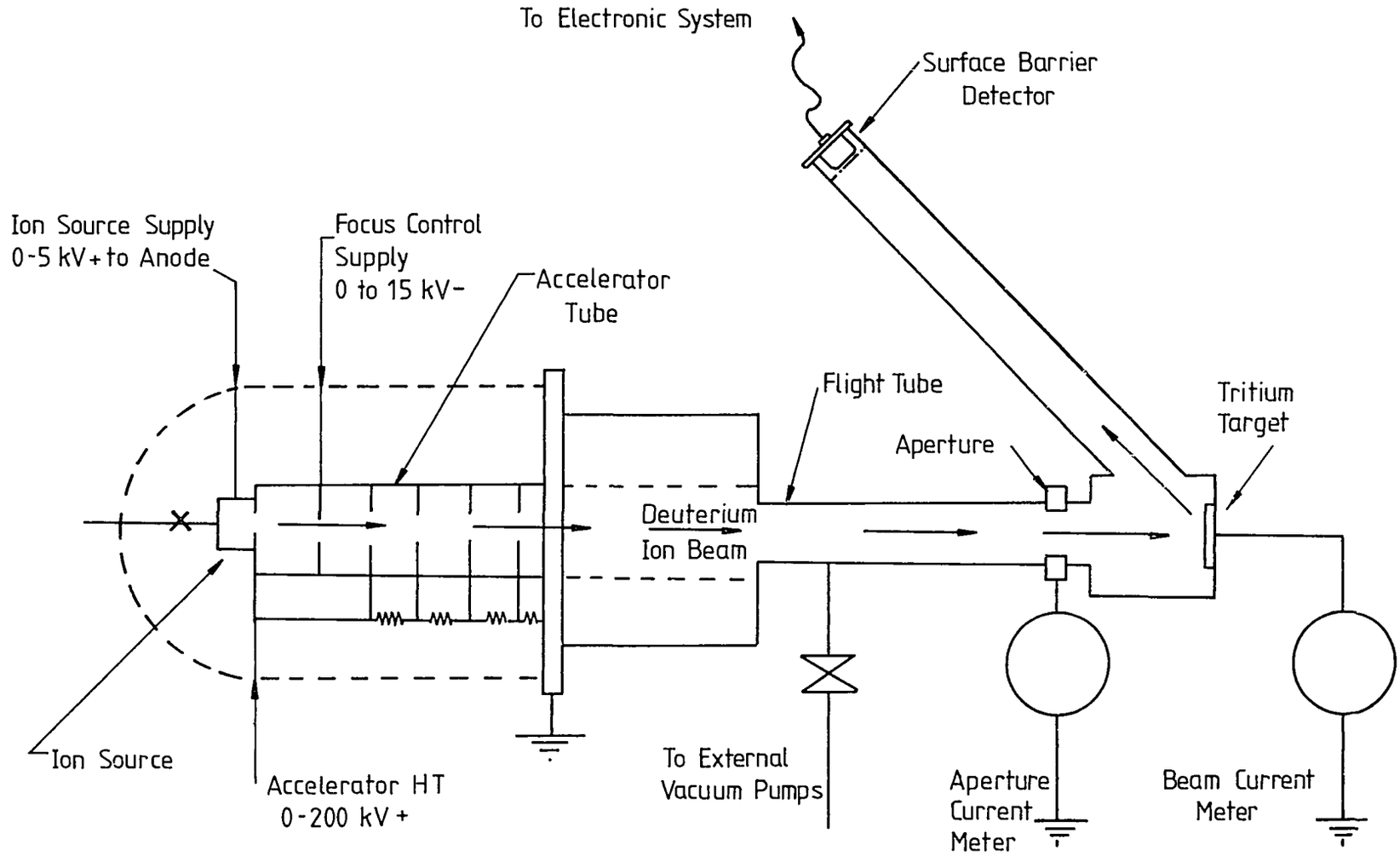

Figure 1 Schematic diagram of accelerator with surface barrier detector

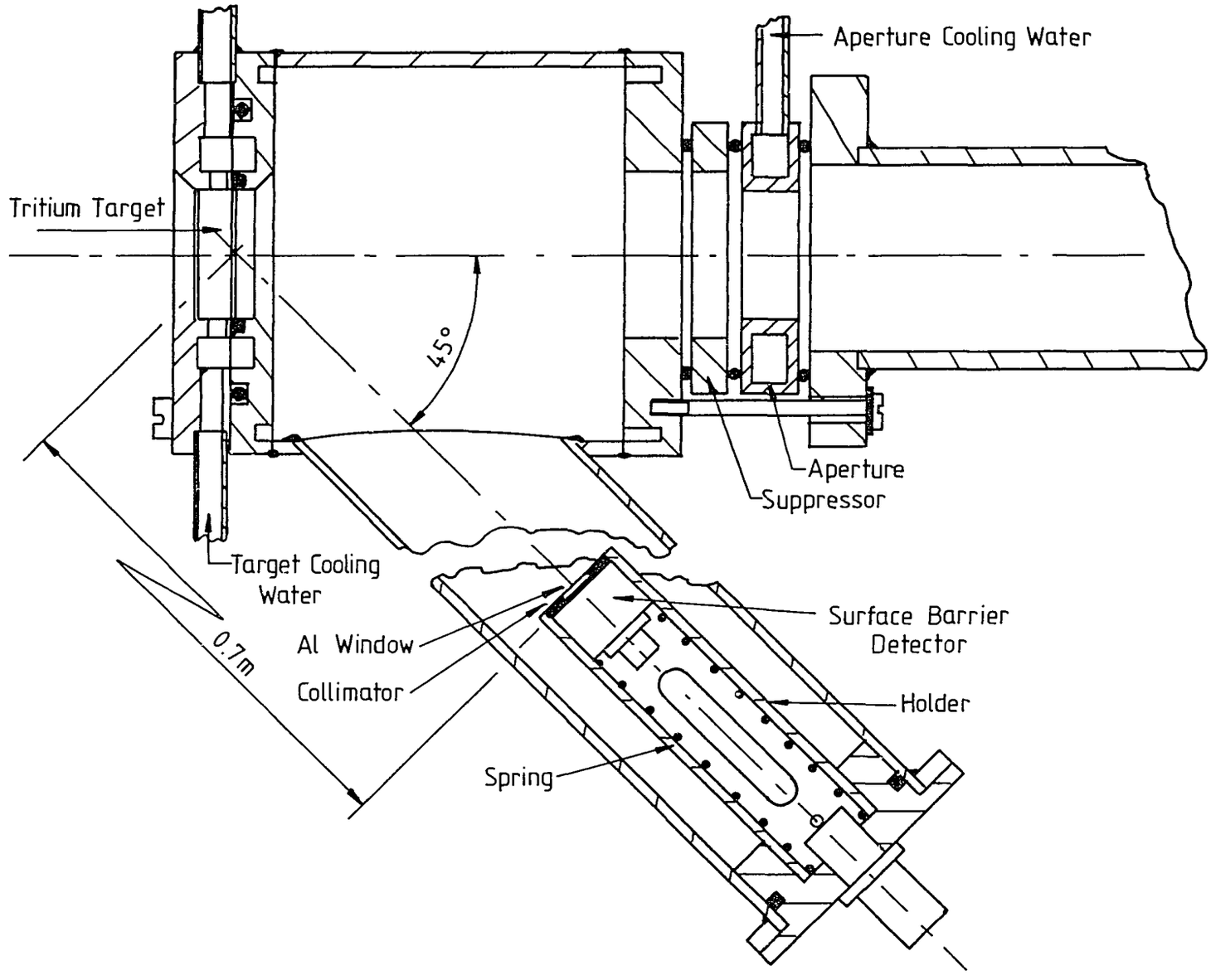

Figure 2 Detail of surface barrier detector mounting

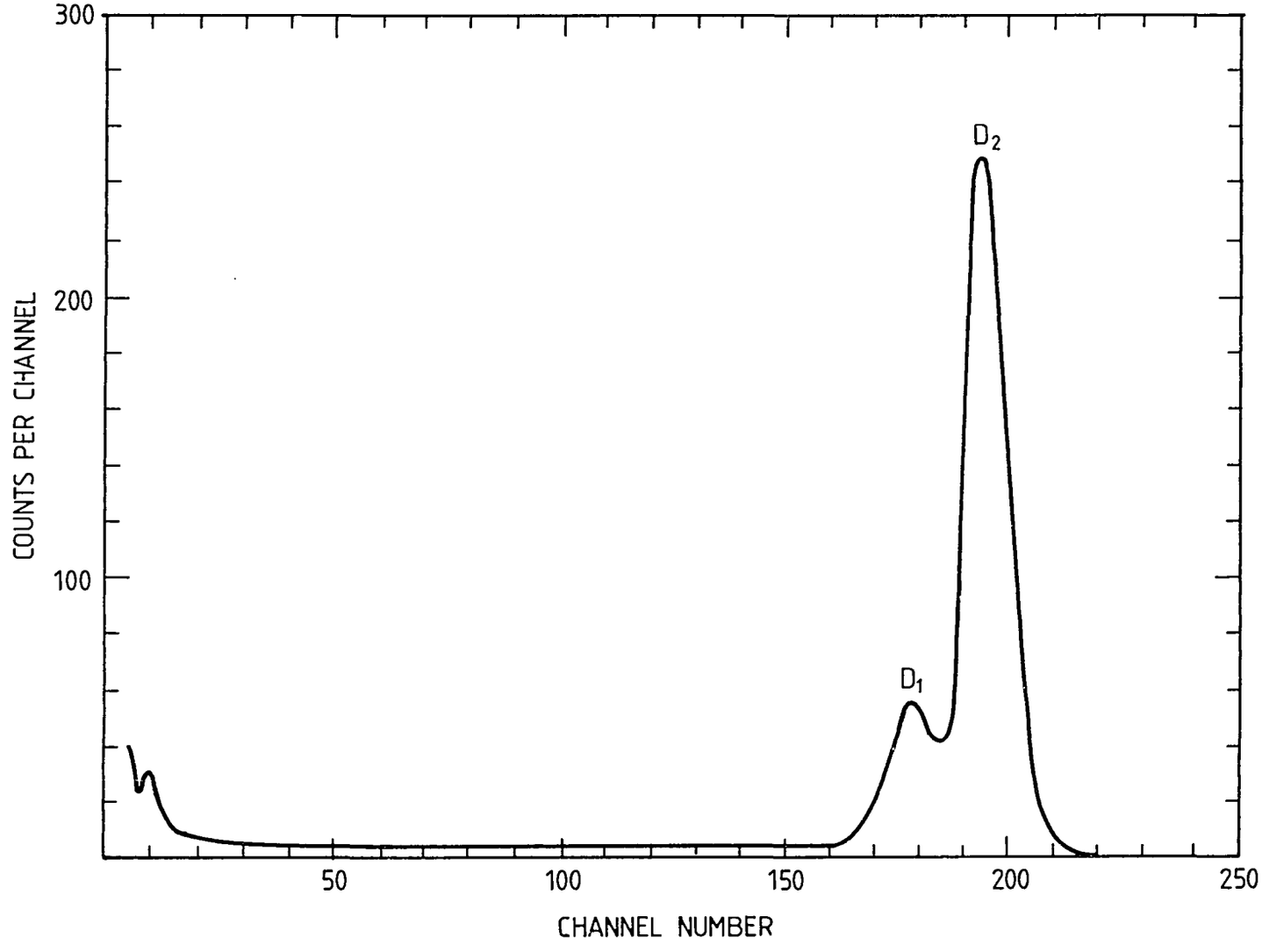

Figure 3 Alpha particle energy spectrum - new target

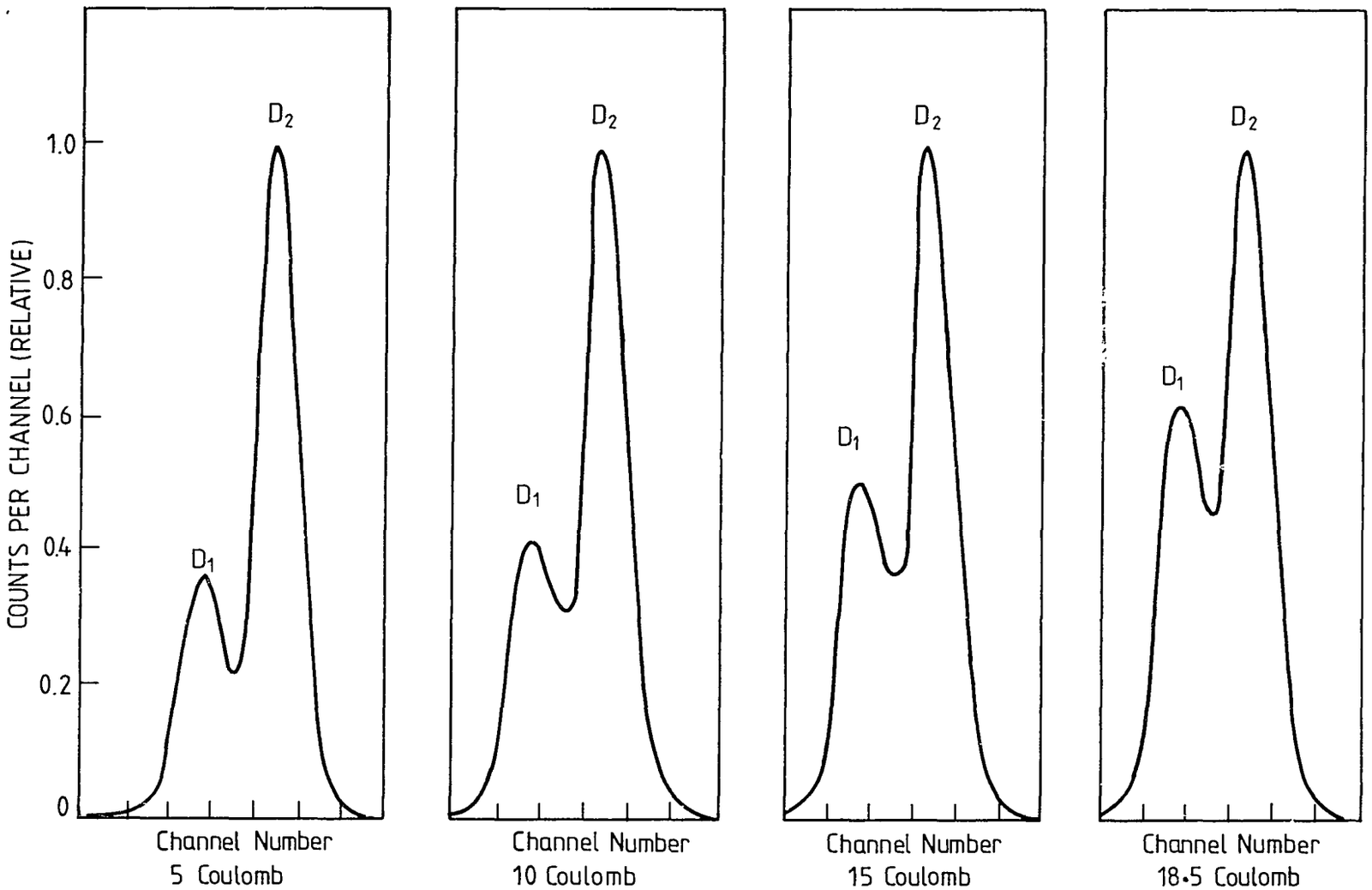

Figure 4 Variation of charged particle spectra with target irradiation (normalised to D_2)

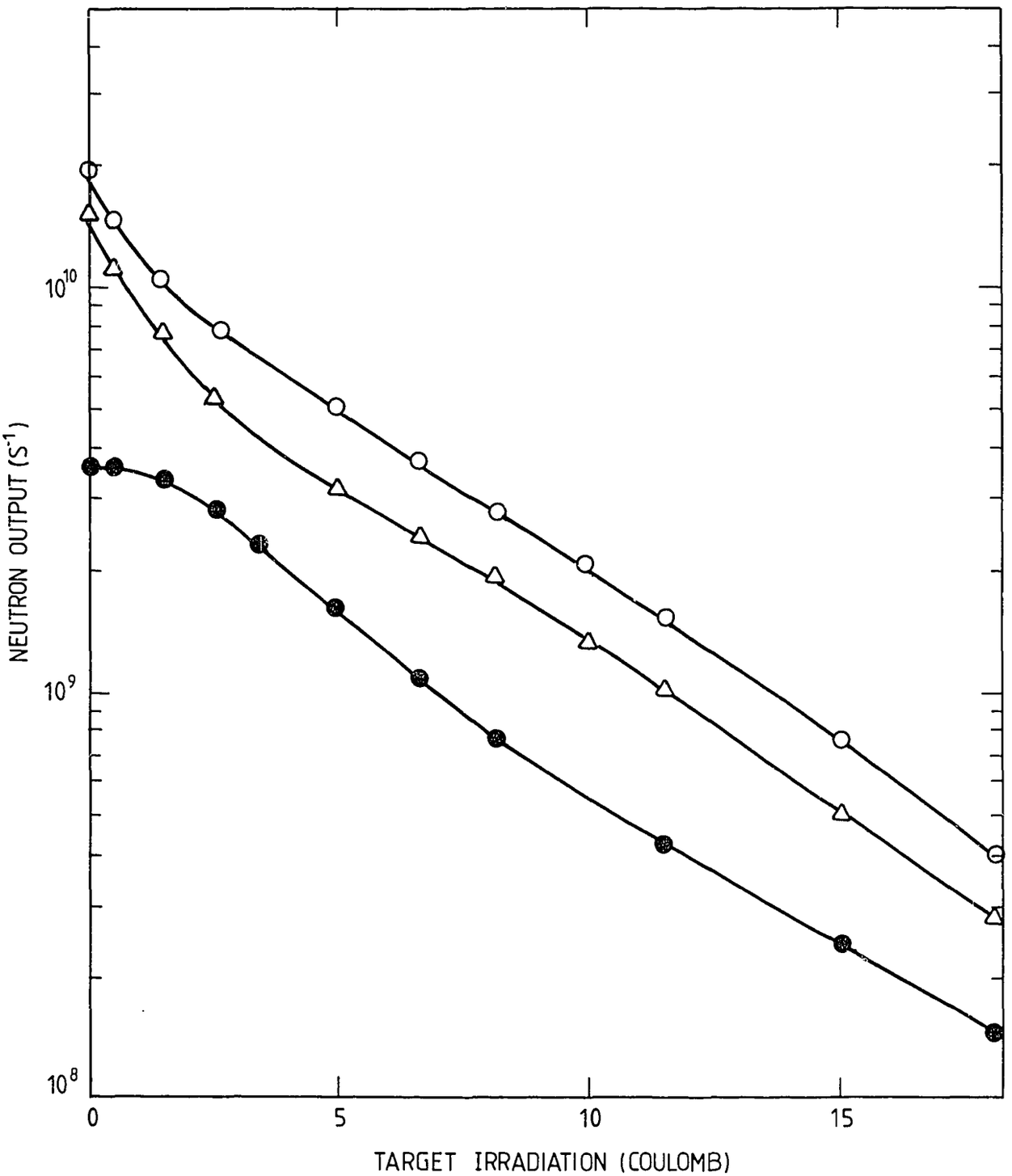

Figure 5 Variation of neutron output with target irradiation